Modeling Optical Interference Effects for Optimization of Electron Emission Properties from Thin Film Semiconductor Photocathodes

D. A. Dimitrov, A. Alexander, C. Huang, N. Moody, V. Pavlenko,
E. Simakov, G. Wang, H. Yamaguchi
Los Alamos National Laboratory, Los Alamos, NM 87545, USA

K. L. Jensen,
University of Maryland, College Park, MD 20741, USA

J. Smedley
SLAC National Accelerator Laboratory, Menlo Park, CA 94025, USA

LA-UR-23-31152

Outline

Motivation: Can we develop models to better understand thin film photcathodes to optimize quantum efficiency (QE), intrinsic emittance, and selection of materials?

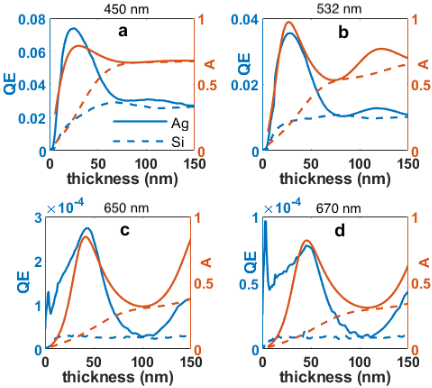

Figure 1: QE ehnancement was demonstrated experimentally (A. Alexander *et al.*, AIP Advances **11**, 065325 (2021) (#), A. Alexander *et al.*, J. Vac. Sci. Technol. B **35**, 022202 (2017)) using thin Cs_3Sb films grown on specific substrates.

Conceptual description of the 3 step model (3SM) of emission.

1. Generation of electron-hole pairs due to absorption of photons.
2. Transient to drift-diffusion charge transport.
3. Electron emission at the vacuum interface.

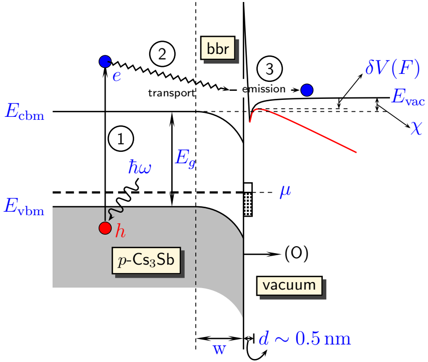

Figure 2: Simplified representation of the 3 steps for electron emission from Cs_3Sb.

Example implementation of a 3SM for diamond in a Monthe Carlo transport framework: Dimitrov *et al.*, J. Appl. Phys. **108**, 073712-1/14 (2010) & Dimitrov *et al.*, J. Appl. Phys. **117**, 055708-1/18 (2015).

Moments model of electron emission properties.

- We are interested in QE here: ratio of number of emitted electrons to the number of photons incident on the photocathode: $QE = \frac{J/q}{I_0/\hbar\omega}$
- QE can be calculated using the moments model (MM) which is similar to the 3SM (see, e.g., K. Jensen, IEEE Trans. Plasma Sci. **46**, 1881 (2018)).
- Moments are averages with a distribution function taking into account absorption ($\mathbb{A}$), transport ($\mathbb{T}$), and emission ($\mathbb{E}$) terms.

Moments: $M_n(k_j) \equiv \langle k_j^n \rangle$

$$M_n(k_j) = (2\pi)^{-3} \int d^3k k_j^n \times \mathbb{E} \times \mathbb{T} \times \mathbb{A}$$

QE from a semi-infinite photcathode:

$$QE = (1 - R(\omega)) \frac{M_1(k_z)}{2M_1(k)|_{D=1,\, f_\lambda=1}}$$

MM of QE for a semi-infinite semiconductor photocathode.

QE expressed as averages over electron energies:

$$QE = (1 - R(\omega)) \frac{\int_{E_a}^{\hbar\omega - E_g} dEE \int_{\sqrt{E_a/E}}^{1} duD(Eu^2)uf_{si}(\omega, E, u)}{2\int_{0}^{\hbar\omega - E_g} dEE \int_0^1 du}$$

- $1 - R(\omega)$ is the fraction of absorbed light intensity ($R(\omega)$ is the photocathode reflectance)
- E_g - energy gap, E_a - electron affinity, $\hbar\omega$ - photon energy
- $u \equiv \cos\theta$, θ - angle of a photo-excited electron relative to the normal of the emission surface
- $D(Eu^2)$ - probability of emission of an electron moving towards the emission surface with parallel kinetic energy Eu^2
- $f_{si}(\omega, E, u)$ photon absorption and transport term for a semi-infinite photocathode
- Main assumptions/simplifications that enable three step types of models are summarized in K. Jensen, IEEE Trans. Plasma Sci. **46**, 1881 (2018)).

Emission probability, absorption, and transport.

- We use a stair step potential barrier with height E_a to calculate emisison probabilites ($E' = E\cos^2(\theta)$):

$$D_{SS}(E') = \frac{4\sqrt{E'(E'-E_a)}}{(\sqrt{E'}-\sqrt{E'-E_a})^2}$$

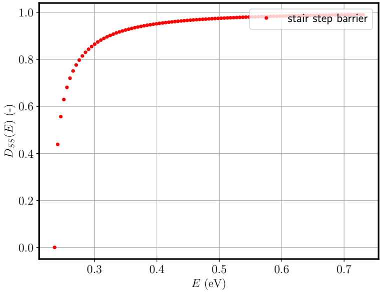

Figure 3: $D_{SS}(E)$ with $E_a = 0.23$ eV.

Absorption and transport: semi-infinite photocathode

$$f_{si}(\omega,\, E,\, \cos\theta) = \frac{\int_0^\infty e^{-x/\delta(\omega) - x/(\lambda(E)\cos\theta)}dx}{\int_0^\infty e^{-x/\delta(\omega)}dx} = \frac{\cos\theta}{\cos\theta + \delta(\omega)/\lambda(E)}$$

$\delta(\omega)$ - absorption length, $\lambda(E)$ - electron mean free path (MFP)

Electron transport in Cs_3Sb is dominated by scattering with polar optical phonons.

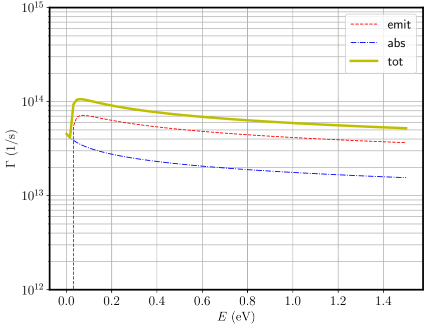

Figure 4: Scattering rates.

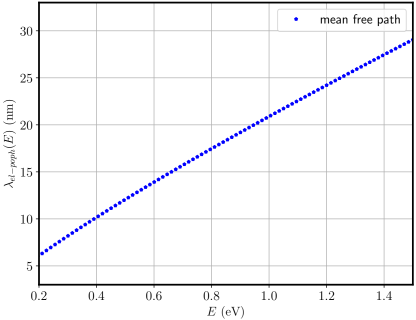

Figure 5: Mean free path.

K. L. Jensen *et al.*, J. Appl. Phys. **105**, 044907 (2008) (*),
P. Gupta *et al.*, J. Appl. Phys. **121**, 215702 (2017).

Electron transport in Cs_2Te is also dominated by scattering with polar optical phonons.

Parameters for electron-phonon scattering are from: G. Adhikari et al., "Monte Carlo Simulation Study of Cs2Te", slides presented at EWPAA 2022 (available on-line) (†).

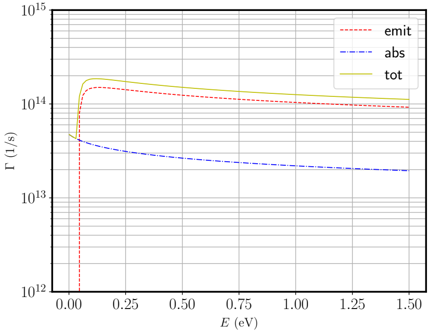

Figure 6: Scattering rates.

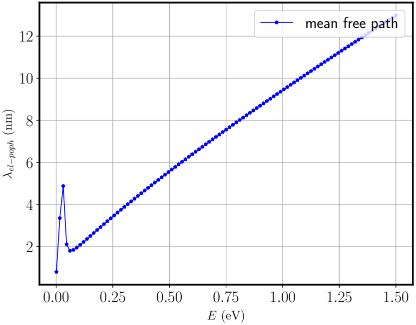

Figure 7: Mean free path.

For modeling Cs_2Te thin films, we used the dielectric fuction to calculate the index of refraction.

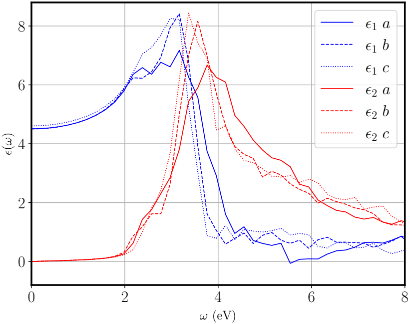

Figure 8: The Cs_2Te dielectric function along main coordinate axes of the crystal structure was obtained from DFT calculations (Gaoxue Wang, LANL).

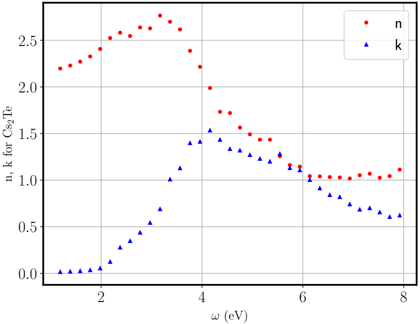

Figure 9: The real and imaginary parts of the Cs_2Te index of refraction was calculated from the DFT dielectric function results.

Optical interference effects in a thin film photocathode

- Light E-field in photocathode: $E_{ph}(x) = E_0(t_1 e^{i\kappa_1 x} + r_1 e^{-i\kappa_1 x})$
- The E-field r_i and t_i coefficients depend on indices of refraction $\hat{n}_i = n_i(\omega) + ik_i(\omega)$ in different material layers and on L.
- For normal light incidence, r_i and t_i are derived in K. L. Jensen *et al.*, J. Appl. Phys. **128**, 115301 (2020).

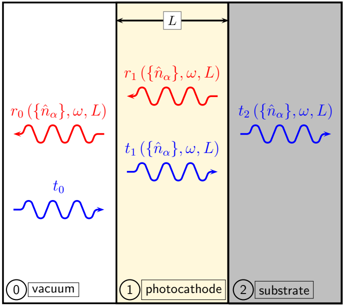

Figure 10: Schematic of incident light on a photocathode thin film of thickness L deposited on a (metal) substrate.

Absorption and transport: thin film photocathode

$$f_{tf}(\omega, E, \cos(\theta)) = \frac{\int_0^L |E_{ph}(x)|^2 e^{-x/(\lambda(E)\cos(\theta))} dx}{\int_0^L |E_{ph}(x)|^2 dx}$$

Extended MM of QE

QE for a thin fim semiconductor photocathode on a substrate.

$$QE = (1 - R_0(\omega) - T_2(\omega)) \frac{\int_{E_a}^{\hbar\omega - E_g} dEE \int_{\sqrt{E_a/E}}^{1} duD(Eu^2)uf_{tf}(\omega, E, u)}{2\int_0^{\hbar\omega - E_g} dEE \int_0^1 du}$$

- $1 - R_0(\omega) - T_2(\omega)$ is the fraction of absorbed light intensity in the photocathode
- $R_0(\omega)$ - vacuum reflectance, $T_2(\omega)$ - substrate transmittance
- R_0 and T_2 depend on photon energy, the complex indices of refraction, and L. (K. L. Jensen *et al.*, J. Appl. Phys. **128**, 115301 (2020).)

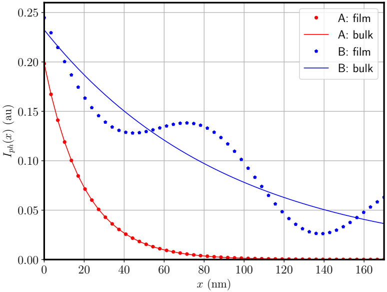

Figure 11: Intensity $I_{ph} \propto |E_{ph}(x)|^2$ for (A) Cs_3Sb on Cu, $\lambda = 532$ nm and (B) CsK_2Sb on Ag, $\lambda = 650$ nm; $L = \lambda/3$.

Optical interference could lead to light absorption increase near the emission surface.

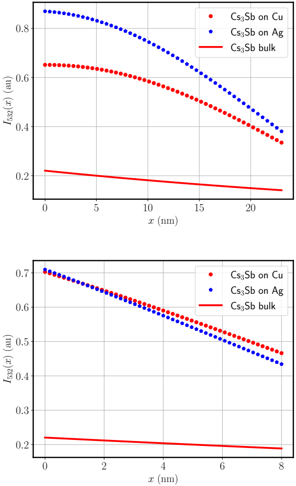

Figure 12: Cs_3Sb, $L = 23$ nm and 8 nm.

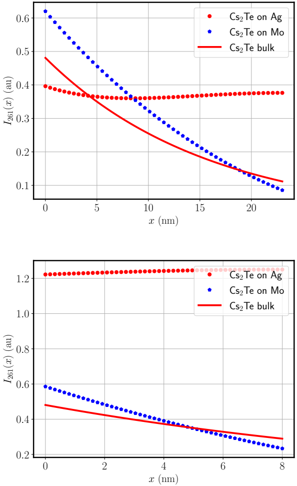

Figure 13: Intensity in Cs_2Te, same L's.

Effect of optical interference in thin films to enhance QE in Cs_3Sb on Ag.

$$p_{semi-inf.}(x) = \frac{e^{-x/\delta(\omega)}dx}{\delta(\omega)}, \quad p_{layer}(x) = \frac{\left|E_{ph}(x)\right|^2 dx}{\int_0^L \left|E_{ph}(x)\right|^2 dx}$$

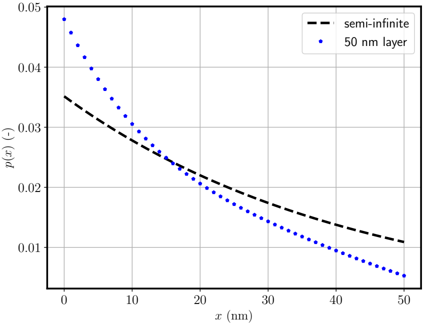

Figure 14: For $\lambda = 532$ nm, photon absorption is enhanced in the thin film, $L = 50$ nm, near the emission surface.

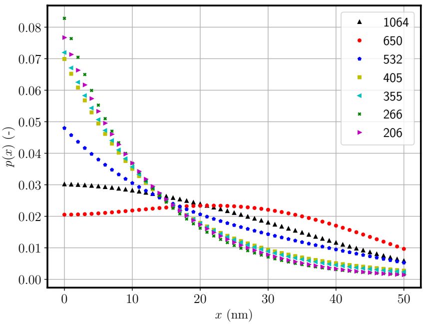

Figure 15: Optical absorption enhancement in a the thin film, $L = 50$ nm, depends on photon wavelength.

Coomparison to QE experimental data from Cs_3Sb on Ag and Si, $\lambda = 670$ nm.

- The electron affinity was set to $E_a = 0.236$ eV and kept at this value for all subsequent calculations.
- The energy gap $E_g = 1.6$ eV is from (*)).
- Complex index of refraction data from Cs_3Sb and Ag is from (*) and (#).
- n and k for Si are from Aspnes and Studna, Phys. Rev. B **27**, 985 (1983).

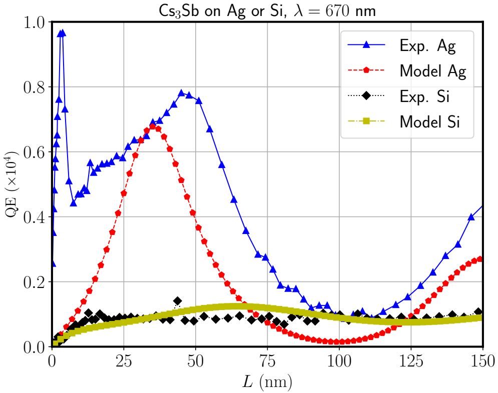

Figure 16: We used experimental data on QE from near emission threshold Cs_3Sb on Ag to set the electron affinity.

Comparison to QE experimental data (#) from Cs_3Sb on Ag and Si, for $\lambda = 450$ nm and 532 nm.

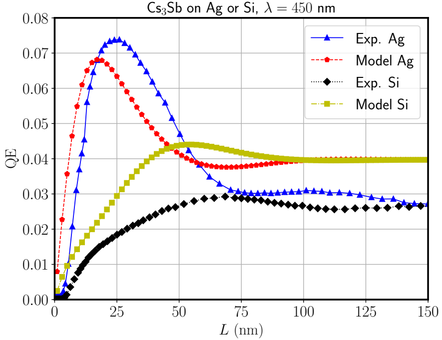

Figure 17: For $\lambda = 450$ nm (2.755 eV), the QE from Cs_3Sb on Ag is highest for Cs_3Sb film thickness near 21 nm.

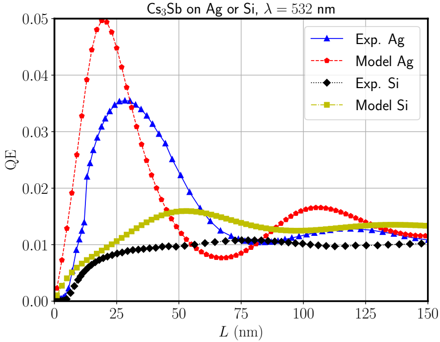

Figure 18: The extended MM for QE shows similar functional behavior with film thickness for both substrates.

Effect of optical interference in Cs_2Te thin films grown on Ag and Mo also lead to enhancement of QE.

For Cs_2Te, we used $E_g = 3.3$ eV and $E_a = 0.25$ eV derived from experimental data (†).

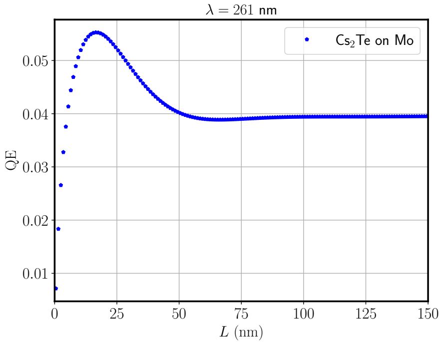

Figure 19: Model calculations of QE vs film thickness for $\lambda = 261$ nm (4.75 eV) show enhancement for both cases.

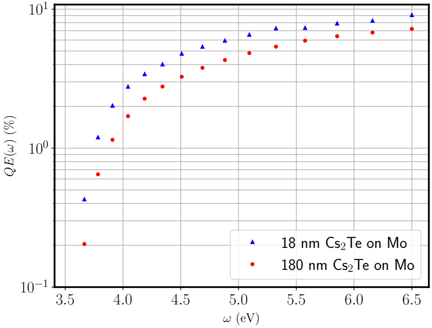

Figure 20: Optical interference enhancement of the QE for Cs_2Te on Mo appears across the spectral response.

3SM for intrinsic emittance from a semiconductor photocathode.

- For electron emission without correlation between location and emission angle, the normalized thermal (intrinsic) emittance per unit beam size (in units of $\mu m/mm$): $\frac{\epsilon_n}{\sigma_x} = \frac{\sqrt{\langle p_x^2 \rangle}}{mc}$.
- For isotropic transverse emission, the mean transverse energy (MTE) is $MTE = m \left\langle v_x^2 \right\rangle = \left\langle p_x^2 \right\rangle / m$.
- This allows to express the normalized emittance through the MTE: $\frac{\epsilon_n}{\sigma_x} = \sqrt{\frac{MTE}{mc^2}}$.
- For emittance, the light interference effects appear only in the $f_{tf}(\omega,\ E,\ \cos(\theta))$ term.

3SM for $\langle p_x^2 \rangle$

$$\frac{\left\langle p_x^2 \right\rangle}{m} = \frac{\int\limits_{E_a}^{\hbar\omega - E_g} dEE \int\limits_{\sqrt{E_a/E}}^{1} duD(Eu^2)(1-u^2)f(\omega, E, u)}{\int_{E_a}^{\hbar\omega - E_g} dE \int_{\sqrt{E_a/E}}^{1} duD(Eu^2)f(\omega, E, u)}$$

Mean transverse energy and intrinsic emittance of electrons emitted from Cs_2Te thin film grown on Mo.

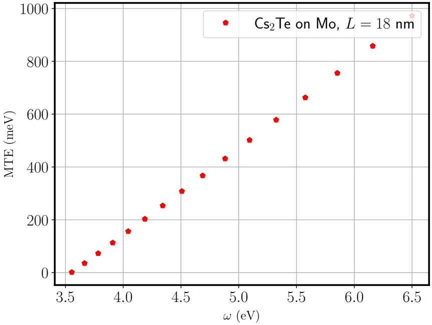

Figure 21: Calculated MTE from an 18 nm Cs_2Te thin film grown on Mo.

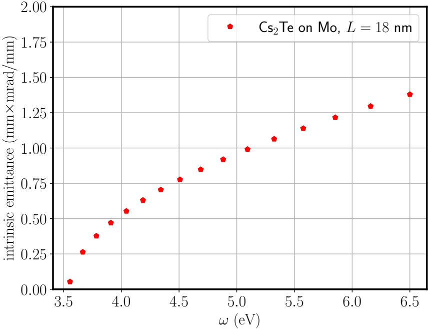

Figure 22: The intrinsic emittance is obtained from the MTE.

The current model does not include temperature effects leading to the MTE (and the intrinsic emittance) going to 0 when the photon energy approaches the emission threshold from above.

Summary

- We implemented an extension to the moments and three step models to calculate QE and MTE from semiconductor thin films grown on substrate materials.
- The model takes into account optical interference effects.
- We applied the model to study QE from Cs_3Sb on Ag and Si compared our results to experimental data.
- The only parameter set in the model was the electron affinity using experimental data on QE near threshold.
- Results from the model on QE vs film thickness at different photon wavelengths recover the observed functional dependance and are in qualitative agreement with the experimental data.
- The model can be used to optimize QE as a function of thin-film thickness and photon wavelength leading to a factor of two or higher QE compared to thick (semi-infinite) Cs_3Sb cathodes.
- We also calculated QE and MTE/emittance from Cs_2Te thin films on Mo and Ag. Optical interference also leads to inrease in QE.

We are considering several future developments to improve the modeling.

- Extend the model by including photocathode material density of states and temperature effects.
- Extend the model to handle electron emission due to back-side laser illumination (transmission mode operation).
- Extend the model to other photocathode and substrate materials - one way is to connect it to a database of material parameters that are used as input to the model.
- Use the extended moments model to implement machine learning approaches to design photocathodes optimized for specific applications.

Acknowledgements

We are grateful to the DOE/NNSA for supporting this work under LANL's LDRD program and the DOE/ARDAP under the LANLE6E7 grant.